Journal of Engineering Mathematics **32:** 281–304, 1997.

The Golden-Ten equations of motion

J.C. DE VOS[1]* and A.A.F. VAN DE VEN[2]
[1] *Co-operation Centre Tilburg and Eindhoven Universities, P.O. Box 90153, 5000 LE Tilburg, The Netherlands*
[2] *Eindhoven University of Technology, Department of Mathematics and Computing Science, P.O. Box 513, 5600 MB Eindhoven, The Netherlands*

Received 21 March 1995; accepted in revised form 11 June 1996

Abstract. Golden Ten is an observation game which is played with a small ball rolling down in a large bowl. This paper describes the motion of the ball in the bowl by means of a deterministic mechanical model, which leads to a set of ordinary second-order differential equations. A first impression of the solution is obtained through a numerical approximation, based on some preliminary estimates. Part of the solution is computed exactly, yielding a simple estimation procedure for the coefficient of air friction, which is one of the two main parameters controlling the system (the other parameter is the angle of inclination). An asymptotic solution method eventually leads to an approximate explicit solution, describing the motion of the ball as an elliptical spiral. One of the conclusions is a simple prediction strategy.

Key words: asymptotic power series, equation of motion, multiple scales, nonlinear differential equation, observation game.

1. Introduction

Golden Ten is a modified version of Roulette. The game is played with a small ball moving in a relatively large drum, at the bottom of which there is a ring with numbered compartments. The main differences with Roulette are that the drum is in fact a smooth, conic bowl in which the ball smoothly spirals down, and secondly that the players do not have to stake before the ball has reached a certain level. Although the players cannot control the motion of the ball, it is claimed that the possibility to observe part of the ball's orbit enables them to make a better than random guess on the outcome. This would imply that Golden Ten is a game of skill, rather than a game of chance.

The main attributes of the game are a small solid ball, made of ivory-like synthetic material, and a big, slightly grooved, uncoated metal drum; Figures 1 and 2 respectively show a top- and a side-view of the drum. At the beginning of the game, the ball is launched from a slit plastic arm at the upper rim of the drum. After rolling a few rounds alongside of the rim, the ball gradually spirals down the drum, towards a ring with twenty-six numbered, equally large compartments. On the surface of the drum two concentric circles have been drawn (as shown in Figure 1). The upper circle is called the *observation ring*, the lower one is the *limit ring*. The players start betting – on one or more possible outcomes – when the ball reaches the observation ring, and the betting must be stopped at the limit ring.

This paper employs a mechanical model to describe the motion of the ball in the drum. The model results in a set of second-order, ordinary differential equations, with a corresponding set of theoretical initial conditions. An exact analytical solution to this system of equations is not available, but a numerical solution based on preliminary estimates from [1], complemented with an asymptotic approximation based on the small values of the system parameters, provide

* Affiliated to Tilburg University, Department of Econometrics.

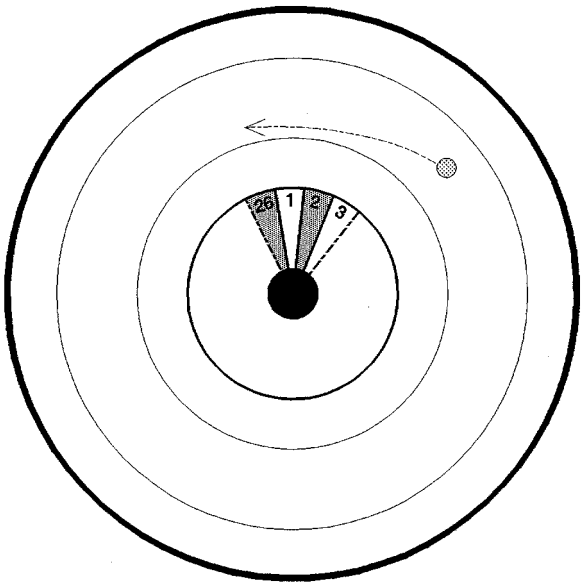

Figure 1. The Golden-Ten drum; top-view.

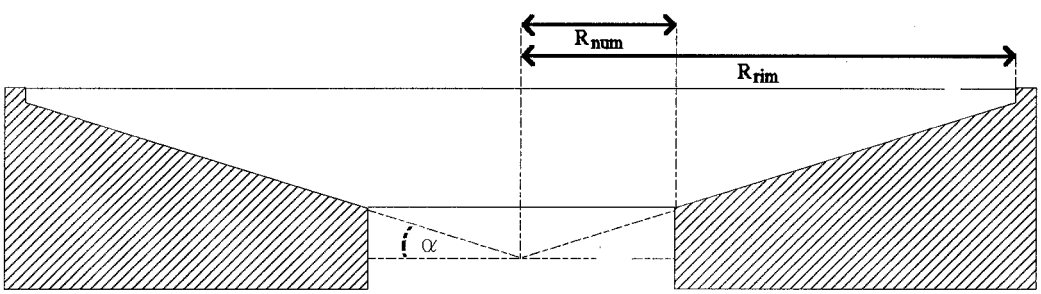

Figure 2. The Golden-Ten drum; side-view.

ample information on the characteristics of the solution. One of the results is a parametrization of the trajectory of the ball as an elliptical spiral, moving down from the rim towards the apex of the drum. This clearly perceptible pattern leads to a simple prediction strategy, of which the yield depends on the validity of the assumptions in the – deterministic – mechanical model.

The system of differential equations can be rewritten in terms of new variables, after which one of the equations directly leads to an exact analytical result. This result provides a means to accurately estimate the unknown value of one of the model parameters, namely the coefficient of air friction. Future research will hopefully render estimates of the remaining unknown values. By then, the analytical results from the current paper – including the asymptotic power series – will serve as a basis for a close comparison of the theoretical solution to empirical data, as supplied by [1]. As has already been indicated by previous research in [2], this comparison will probably lead to an extension of the mechanical model with random factors, the nature of which will have to be determined through further research.

2. The mechanical model

The most natural model to describe the motion of the ball is a three-dimensional rigid-body model, but, before such a model can be constructed, we have to make some basic assumptions:

(a) the ball is a uniform sphere;
(b) the drum is rotationally symmetric;
(c) the surface of the drum – including that of the rim – is so smooth that the ball rolls without bouncing, but on the other hand so rough that the ball (after two or three revolutions along the rim) rolls without slipping;
(d) the motion of the ball is completely deterministic, i.e. no random factors are included.

No assumptions are made for the – preferably – horizontal position of the drum, i.e. we allow for a slightly tilted position. We denote the angle over which the drum is tilted with β. The radius of the ball is a, that of the rim is R_{rim}, whereas R_{num} denotes the radius of the numbered ring. The angle of inclination of the conical drum surface is α (as in Figure 2). Note that $0 < \alpha \ll \pi/2$ and $0 \leqslant \beta \ll \alpha$.

We introduce a moving rectangular coordinate system $\{O\boldsymbol{e}_1\boldsymbol{e}_2\boldsymbol{e}_3\}$ to describe the motion of the ball on the surface of the drum (see Figures 3 and 4). The origin O coincides with the apex of the drum, $\boldsymbol{e}_1$ points in the direction from O to P (being the point of contact between the ball and the drum) and $\boldsymbol{e}_3$ is parallel to the drum surface normal in P. The rotation of the three coordinate axes can thus be written as

$$\dot{\boldsymbol{e}}_i = \frac{\mathrm{d}}{\mathrm{d}t}\boldsymbol{e}_i = \boldsymbol{\Omega} \times \boldsymbol{e}_i, \tag{1}$$

where $\boldsymbol{\Omega}$ represents the angular velocity. Calling φ the angle of rotation of $\boldsymbol{e}_1$ about the central axis of the drum, we obtain

$$\boldsymbol{\Omega} = \dot{\varphi} \sin\alpha\, \boldsymbol{e}_1 + \dot{\varphi} \cos\alpha\, \boldsymbol{e}_3. \tag{2}$$

The position $\boldsymbol{x}_o$ of the centre of the ball o, with respect to O, can be described by

$$\boldsymbol{x}_o = r\boldsymbol{e}_1 + a\boldsymbol{e}_3, \tag{3}$$

where r is the distance from O to P. The velocity $\boldsymbol{v}_o$ of o is the time derivative of $\boldsymbol{x}_o$, so it equals

$$\boldsymbol{v}_o = \dot{\boldsymbol{x}}_o = \dot{r}\boldsymbol{e}_1 + r\dot{\boldsymbol{e}}_1 + a\dot{\boldsymbol{e}}_3. \tag{4}$$

By substituting (1) in (4), and introducing

$$R = r\cos\alpha - a\sin\alpha, \tag{5}$$

we obtain

$$\boldsymbol{v}_o = \dot{r}\boldsymbol{e}_1 + (r\dot{\varphi}\cos\alpha - a\dot{\varphi}\sin\alpha)\boldsymbol{e}_2 = \frac{\dot{R}}{\cos\alpha}\boldsymbol{e}_1 + R\dot{\varphi}\boldsymbol{e}_2. \tag{6}$$

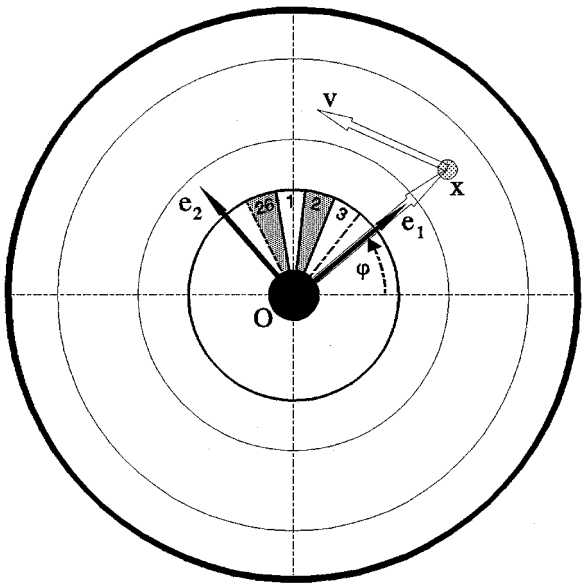

Figure 3. The moving frame $\{O\boldsymbol{e}_1\boldsymbol{e}_2\boldsymbol{e}_3\}$; top-view.

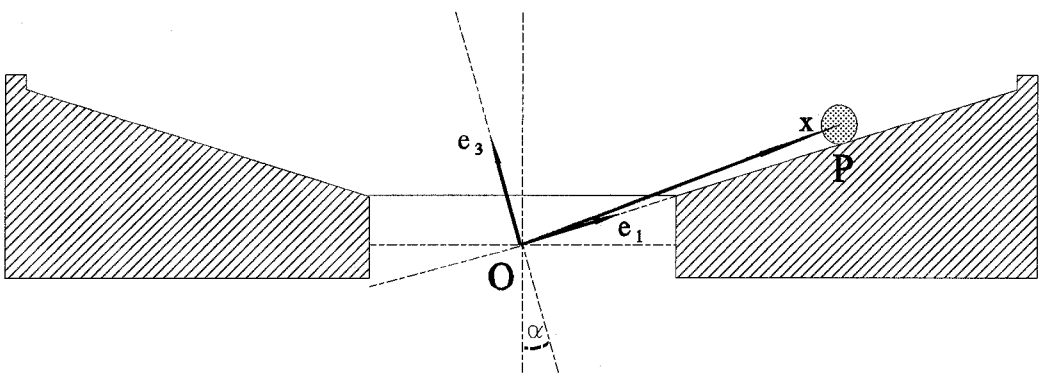

Figure 4. The moving frame $\{O\boldsymbol{e}_1\boldsymbol{e}_2\boldsymbol{e}_3\}$; side-view.

Likewise, the acceleration of o is

$$\begin{aligned}\dot{\boldsymbol{v}}_o &= \frac{\ddot{R}}{\cos\alpha}\boldsymbol{e}_1 + \frac{\dot{R}}{\cos\alpha}\dot{\boldsymbol{e}}_1 + \dot{R}\dot{\varphi}\boldsymbol{e}_2 + R\ddot{\varphi}\boldsymbol{e}_2 + R\dot{\varphi}\dot{\boldsymbol{e}}_2 \\ &= \left(\frac{\ddot{R}}{\cos\alpha} - R\dot{\varphi}^2\cos\alpha\right)\boldsymbol{e}_1 + (R\ddot{\varphi} + 2\dot{R}\dot{\varphi})\boldsymbol{e}_2 + R\dot{\varphi}^2\sin\alpha\boldsymbol{e}_3. \qquad (7)\end{aligned}$$

According to assumption c, the ball purely rolls; hence the instantaneous velocity $\boldsymbol{v}_P$ of P is zero. With $\boldsymbol{\omega}$ denoting the angular velocity of the ball, this implies

$$\boldsymbol{0} = \boldsymbol{v}_P = \boldsymbol{v}_o + \boldsymbol{\omega} \times (-a\boldsymbol{e}_3). \qquad (8)$$

Substitution of (6) in (8) yields

$$\boldsymbol{\omega} = -\frac{R\dot{\varphi}}{a}\boldsymbol{e}_1 + \frac{\dot{R}}{a\cos\alpha}\boldsymbol{e}_2 + \dot{\psi}\boldsymbol{e}_3, \tag{9}$$

where $\dot{\psi}$ denotes the third component of $\boldsymbol{\omega}$, which is called the *spin*. We obtain the time derivative of $\boldsymbol{\omega}$ by differentiating (9), and substituting (1) in the result

$$\begin{aligned}\dot{\boldsymbol{\omega}} &= -\frac{\dot{R}\dot{\varphi} + R\ddot{\varphi}}{a}\boldsymbol{e}_1 - \frac{R\dot{\varphi}}{a}\dot{\boldsymbol{e}}_1 + \frac{\ddot{R}}{a\cos\alpha}\boldsymbol{e}_2 + \frac{\dot{R}}{a\cos\alpha}\dot{\boldsymbol{e}}_2 + \ddot{\psi}\boldsymbol{e}_3 + \dot{\psi}\dot{\boldsymbol{e}}_3 \\ &= -\frac{R\ddot{\varphi} + 2\dot{R}\dot{\varphi}}{a}\boldsymbol{e}_1 + \left(\frac{\ddot{R} - R\dot{\varphi}^2\cos^2\alpha}{a\cos\alpha} - \dot{\varphi}\dot{\psi}\sin\alpha\right)\boldsymbol{e}_2 + \left(\frac{\dot{R}\dot{\varphi}\tan\alpha}{a} + \ddot{\psi}\right)\boldsymbol{e}_3. \end{aligned} \tag{10}$$

The equations of motion are implicitly contained in the law of momentum and that of moment of momentum (consult *e.g.* [3], Ch. 8). With m representing the mass of the ball, and $\boldsymbol{F}$ the total force acting on the ball, the first law reads

$$m\dot{\boldsymbol{v}}_o = \boldsymbol{F} \tag{11}$$

and the second states

$$I\dot{\boldsymbol{\omega}} = \boldsymbol{M}, \tag{12}$$

with I representing the central moment of inertia – so $I = \frac{2}{5}ma^2$ – and $\boldsymbol{M}$ being the momentum about o. Before we can elaborate these equations by writing them out in components in the $\{O\boldsymbol{e}_1\boldsymbol{e}_2\boldsymbol{e}_3\}$ system, we must first specify $\boldsymbol{F}$ and $\boldsymbol{M}$. Four distinct forces act on the ball: the normal force $\boldsymbol{F}_n$, the frictional force (or dry friction) $\boldsymbol{F}_d$, the resistive force $\boldsymbol{F}_a$ (due to air friction) and the gravitational force $\boldsymbol{F}_g$. These forces combine into

$$\boldsymbol{F}_n + \boldsymbol{F}_d + \boldsymbol{F}_a + \boldsymbol{F}_g = \boldsymbol{F}. \tag{13}$$

Note that the forces $\boldsymbol{F}_n, \boldsymbol{F}_a$ and $\boldsymbol{F}_g$ act in o, whereas the line of action for $\boldsymbol{F}_d$ is through P, in the e_1e_2-plane. Hence only $\boldsymbol{F}_d$ contributes to the momentum about o.

The normal force can simply be written as

$$\boldsymbol{F}_n = N\boldsymbol{e}_3, \tag{14}$$

where N is a nonnegative scalar. Likewise, the frictional force – which is tangent to the drum surface in P – is given by

$$\boldsymbol{F}_d = D_1\boldsymbol{e}_1 + D_2\boldsymbol{e}_2. \tag{15}$$

The resistive force $\boldsymbol{F}_a$ is due to the air friction the ball experiences on account of the translation. Since this force is directed opposite to $\boldsymbol{v}_o$ and its magnitude depends on v_o, we write

$$\boldsymbol{F}_a = -\mathcal{F}(v_o)\boldsymbol{v}_o = -\mathcal{F}(v_o)\left(\frac{\dot{R}}{\cos\alpha}\boldsymbol{e}_1 + R\dot{\varphi}\boldsymbol{e}_2\right), \tag{16}$$

where $\mathcal{F}(v_o)$ is a simple function of

$$v_o = \|\boldsymbol{v}_o\| = \sqrt{(\dot{R}\cos^{-1}\alpha)^2 + (R\dot{\varphi})^2}, \tag{17}$$

somewhere in between a constant and a linear function. In case of a freely moving sphere, and for high Reynolds numbers, the friction force is a pure pressure drag. This drag is quadratic in v_o and of the order of $\frac{1}{2}\rho {V_o}^2 C_d\,\pi a^2$, where ρ is the density of air, V_o a characteristic velocity, and C_d the drag coefficient, with $C_d \approx 1$ (cf. [4], Sect. 1.5, or [5], Sect. 40). For $V_o \approx 0{\cdot}5\,\mathrm{m/sec},\ \rho \approx 1{\cdot}2\,\mathrm{kg/m^3}$, and $a = 0{\cdot}0175\,\mathrm{m}$, this yields a magnitude for $\boldsymbol{F}_a$ of about $1{\cdot}5 \times 10^{-4}\,\mathrm{N}$. This is, at least in order of magnitude, in correspondence with values of the resistive force found in our experiments (see Section 3), which are of the order of $3 \times 10^{-4}\,\mathrm{N}$. A linear viscous model, for low Reynolds numbers, would (cf. [4], Sect. 7.6) yield $\boldsymbol{F}_a \sim \eta V_o a C_d$ (η: viscosity of air), which is of the order of 10^{-7}, and thus much lower than the observed values. In the light of our experimental results we favour the quadratic model (yielding a linear $\mathcal{F}(v_o)$), although the ball is not free here, but rolls over a solid surface. However, the range of velocities traversed in practice is limited, and a linear model (having constant $\mathcal{F}(v_o)$) will probably also suffice. In Section 3 we will consider both options, and compare the results.

Considering the gravitational force, we know that it would be directed along the central axis of the drum if the position of the drum were exactly horizontal (the ideal case). We here assume that the drum is tilted about a small angle β, and that the plane of inclination is rotated about an angle φ_β – with $\varphi_\beta \in [0, 2\pi)$ – so that $\boldsymbol{F}_g$ takes the form

$$\begin{aligned}\boldsymbol{F}_g = &- mg(\cos(\varphi-\varphi_\beta)\cos\alpha\sin\beta + \sin\alpha\cos\beta)\boldsymbol{e}_1 + mg\sin(\varphi-\varphi_\beta)\sin\beta\boldsymbol{e}_2 \\ &+ mg(\cos(\varphi-\varphi_\beta)\sin\alpha\sin\beta - \cos\alpha\cos\beta)\boldsymbol{e}_3,\end{aligned} \tag{18}$$

where g represents the acceleration of gravity. Since β is extremely small, the component of the gravitational force in the plane of the drum is of the order $F_g \approx mg\sin\alpha \approx 3 \times 10^{-2}\,\mathrm{N}$, whereas the order of the centrifugal force is $F_c \approx m{V_o}^2/R \approx 2 \times 10^{-2}\,\mathrm{N}$. Hence, F_g and F_c are of the same order of magnitude, but $F_a = \|\boldsymbol{F}_a\|$ is much smaller than both F_g and F_c. Hence it is possible to introduce a small parameter in the form of the quotient of F_a and either F_g or F_c. We will return to this subject in Section 4.

The last term to be expressed in $\{\boldsymbol{e}_1\boldsymbol{e}_2\boldsymbol{e}_3\}$ coordinates is the total momentum $\boldsymbol{M}$, where $\boldsymbol{M}$ is composed of two parts: the momentum $\boldsymbol{M}_d$ caused by the frictional force $\boldsymbol{F}_d$, and the rolling resistance $\boldsymbol{M}_r$ which is assumed to be proportional to the spin (rolling resistance due to the in-plane rotations ω_1 and ω_2 is neglected). So

$$\boldsymbol{M} = \boldsymbol{M}_d + \boldsymbol{M}_r \tag{19}$$

with

$$\boldsymbol{M}_d = -a\boldsymbol{e}_3 \times \boldsymbol{F}_d = aD_2\boldsymbol{e}_1 - aD_1\boldsymbol{e}_2 \tag{20}$$

and

$$\boldsymbol{M}_r = -Ih\dot{\psi}\boldsymbol{e}_3, \tag{21}$$

where h is a friction coefficient. From (3), (6) and (9), we find that the motion of the ball is completely determined by the three variables R, φ and $\dot{\psi}$. By writing (11) and (12) out in

components in the $\{O\boldsymbol{e}_1\boldsymbol{e}_2\boldsymbol{e}_3\}$ system, and by eliminating the unknowns N, D_1 and D_2, we obtain (with $f(v_o)$ denoting $\mathcal{F}(v_o)/m$)

$$\begin{aligned}
\ddot{R} &= -\frac{5}{7}f(v_o)\dot{R} + R\dot{\varphi}^2\cos^2\alpha + \frac{2a}{7}\dot{\varphi}\dot{\psi}\cos\alpha\sin\alpha \\
&\quad -\frac{5g}{7}\cos\alpha(\cos\alpha\sin\beta\cos(\varphi-\varphi_\beta)+\sin\alpha\cos\beta), \\
\ddot{\varphi} &= -\frac{5}{7}f(v_o)\dot{\varphi} - 2R^{-1}\dot{R}\dot{\varphi} + \frac{5g}{7}R^{-1}\sin\beta\sin(\varphi-\varphi_\beta), \\
\ddot{\psi} &= -h\dot{\psi} - \frac{1}{a}\dot{R}\dot{\varphi}\tan\alpha.
\end{aligned} \tag{22}$$

The above system of differential equations is to be completed with a set of initial conditions. We derive these conditions by again using assumption c: when the ball is rolling along the rim (see Figure 5), we know that the instantaneous velocity $\boldsymbol{v}_Q$ of Q (being the point of contact between rim and ball) is equal to zero, hence

$$\mathbf{0} = \boldsymbol{v}_Q = \boldsymbol{v}_o + \boldsymbol{\omega}\times a(\cos\alpha\boldsymbol{e}_1 - \sin\alpha\boldsymbol{e}_3). \tag{23}$$

By substituting equations (6) and (9) in (23), we find

$$\mathbf{0} = \frac{\dot{R}(1-\sin\alpha)}{\cos\alpha}\boldsymbol{e}_1 + \{a\dot{\psi}\cos\alpha + R\dot{\varphi}(1-\sin\alpha)\}\boldsymbol{e}_2 - \dot{R}\boldsymbol{e}_3. \tag{24}$$

At $t=0$ the ball leaves the rim; from (24) we conclude that at this time the ball momentarily moves in a circular orbit ($\ddot{R}(0)=\dot{R}(0)=0$), with radius $R(0)=R_{\text{rim}}-a$. Furthermore we may choose $\varphi(0)$ arbitrarily, so we have $\varphi(0)=\varphi_0$. To find $\dot{\varphi}(0)$ and $\dot{\psi}(0)$, we combine the second component in (24) with the first equation in (22), whence

$$\begin{aligned}
&R(0) = R_{\text{rim}} - a, \qquad \dot{R}(0) = 0, \\
&\varphi(0) = \varphi_0, \qquad \dot{\varphi}(0) = \sqrt{\frac{5g(\sin\alpha\cos\beta + \cos\alpha\sin\beta\cos(\varphi_0-\varphi_\beta))}{R(0)(7\cos\alpha - 2\tan\alpha(1-\sin\alpha))}}, \\
&\dot{\psi}(0) = -\frac{1-\sin\alpha}{a\cos\alpha}R(0)\dot{\varphi}(0).
\end{aligned} \tag{25}$$

At this point we have derived a system of three nonlinear second-order differential equations, and a corresponding set of initial conditions. This system, represented by (22) and (25), completely determines the motion of the ball in the drum. But, unfortunately, it does not seem to admit any standard analytical solution method.

3. Numerical solutions

Any system of second-order differential equations can be rewritten as a system of first-order differential equations by introducing some additional variables. To this end, we define

$$x_1 = R, \qquad x_2 = \dot{R}, \qquad x_3 = \varphi - \varphi_\beta, \qquad x_4 = \dot{\varphi}, \qquad x_5 = \dot{\psi} \tag{26}$$

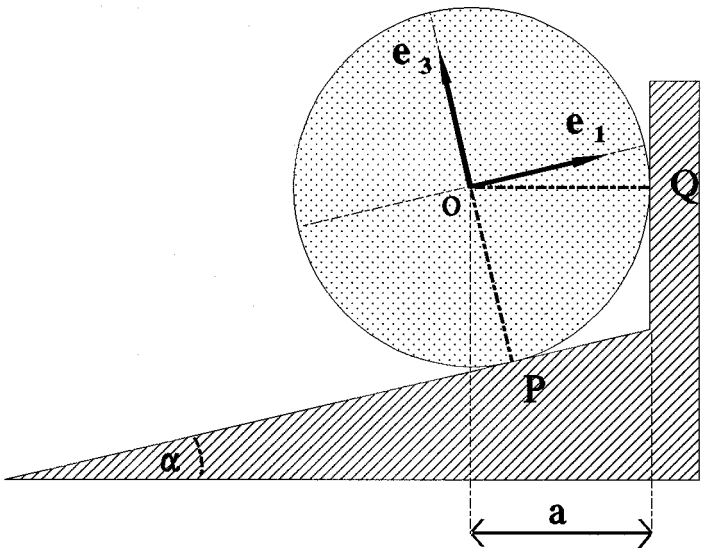

Figure 5. The ball rolling along the rim.

and regard these variables as components of the five-vector

$$\boldsymbol{x}(t) = (x_1(t), x_2(t), x_3(t), x_4(t), x_5(t)). \tag{27}$$

With these new variables, the equations of motion in (22) can be rewritten as

$$\begin{aligned}
\dot{x}_1 &= x_2,\\
\dot{x}_2 &= -\frac{5}{7} f(v_o) x_2 + x_1 {x_4}^2 \cos^2\alpha + \frac{2a}{7} x_4 x_5 \cos\alpha \sin\alpha\\
&\quad -\frac{5g}{7}(\cos\alpha \sin\beta \cos x_3 + \sin\alpha \cos\beta)\cos\alpha,\\
\dot{x}_3 &= x_4,\\
\dot{x}_4 &= -\frac{5}{7} f(v_o) x_4 - 2{x_1}^{-1} x_2 x_4 + \frac{5g}{7} {x_1}^{-1} \sin\beta \sin x_3,\\
\dot{x}_5 &= -h x_5 - \frac{1}{a} x_2 x_4 \tan\alpha,
\end{aligned} \tag{28}$$

where

$$v_o = \sqrt{(x_2 \cos^{-1}\alpha)^2 + (x_1 x_4)^2}. \tag{29}$$

Likewise, with

$$x_{0i} = x_i(0), \quad i \in \{1, \ldots, 5\}, \tag{30}$$

the initial conditions in (25) can be transformed into

$$\begin{aligned} x_{01} &= R_{\text{rim}} - a, \qquad x_{02} = 0, \\ x_{03} &= 0, \qquad x_{04} = \sqrt{\frac{5g(\sin\alpha\cos\beta + \cos\alpha\sin\beta)}{(7\cos\alpha - 2\tan\alpha(1-\sin\alpha))}}{x_{01}}^{-1/2}, \\ x_{05} &= -\frac{1-\sin\alpha}{a\cos\alpha}x_{01}x_{04}, \end{aligned} \tag{31}$$

where the value of $\varphi_0 - \varphi_\beta$ has been set to zero, for the sake of simplicity. We can solve this type of differential equation by using a Runge-Kutta method. We choose the numerical values of the system parameters in (28) and (31) as follows. Since the positioning of the Golden-Ten table must be done very carefully, the position of the drum will be close to horizontal, leaving at most a very small value for β. Therefore we will, in our present calculations, assume

$$\beta = \varphi_\beta = 0. \tag{32}$$

The dimensions of the drum and the ball are supplied by [1], from which we obtain

$$m = 0{\cdot}0383\,\text{kg}, \qquad a = 0{\cdot}0175\,\text{m}, \tag{33}$$

$$R_{\text{rim}} = 0{\cdot}487\,\text{m}, \qquad R_{\text{num}} = 0{\cdot}205\,\text{m}, \qquad \alpha = 0{\cdot}0831\,\text{rad} \tag{34}$$

and

$$g = 9{\cdot}81\,\text{m/sec}^2. \tag{35}$$

The values (32–35) lead to the following initial conditions

$$\begin{aligned} &x_{01} = 0{\cdot}470\,\text{m}, \qquad x_{02} = x_{03} = 0, \\ &x_{04} = 1{\cdot}13\,\text{rad/sec}, \qquad x_{05} = -28\,\text{rad/sec}. \end{aligned} \tag{36}$$

This leaves us with the unknown friction coefficient h and the unknown friction function f. As a start, we neglect the resistive force due to spin[1], thus assuming

$$h = 0. \tag{37}$$

As was already explained in Section 2, we have two options for the air resistance: a resistive force directly proportional to the speed v_o, in which case

$$f(v_o) = f_l, \tag{38}$$

or a purely quadratic model, implying

$$f(v_o) = f_q v_o. \tag{39}$$

[1] It seems to us that this point needs further study. We plan to do this in subsequent work, but for the time being we leave it at this approximation.

Until further notice, we consider both models to be equally acceptable, so we employ them both.

At final time t_f, when the ball hits the numbered ring, we have

$$x_1(t_f) = R_{\text{num}} \tag{40}$$

which allows us to estimate t_f by utilizing the experimental data from [1]. From orbit T11B21 – which is one of the smoothest orbits, and therefore serves as an example – we obtain the value

$$\hat{t}_f = 116\,\text{sec}. \tag{41}$$

We can now determine the two coefficients f_l and f_q by running two Runge-Kutta procedures (one for each friction model) for varying values of f_l and f_q, meanwhile continually checking on condition (40), with t_f substituted by $\hat{t}_f$. This method eventually yields the rough estimates

$$\widehat{f_l} = 0{\cdot}015\,\text{sec}^{-1}, \tag{42}$$

and

$$\widehat{f_q} = 0{\cdot}035\,\text{m}^{-1}. \tag{43}$$

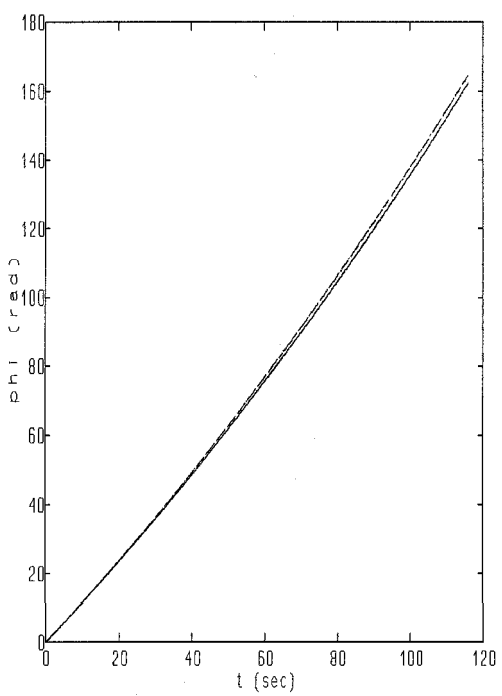

Figure 6. Total angle φ as function of time t.

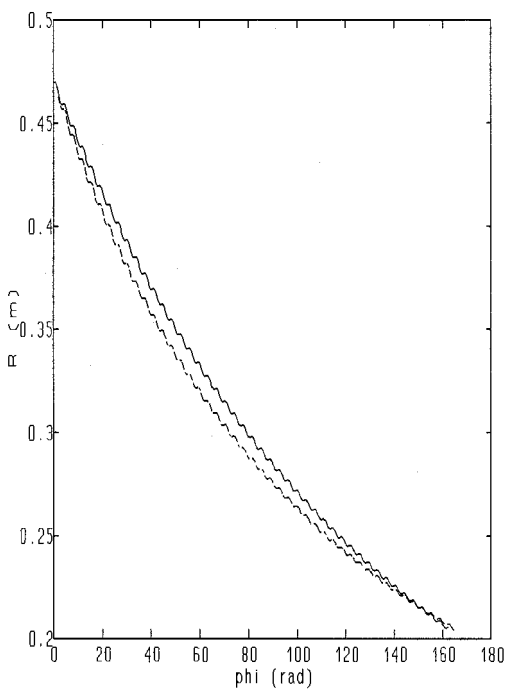

Figure 7. Radius R as function of φ.

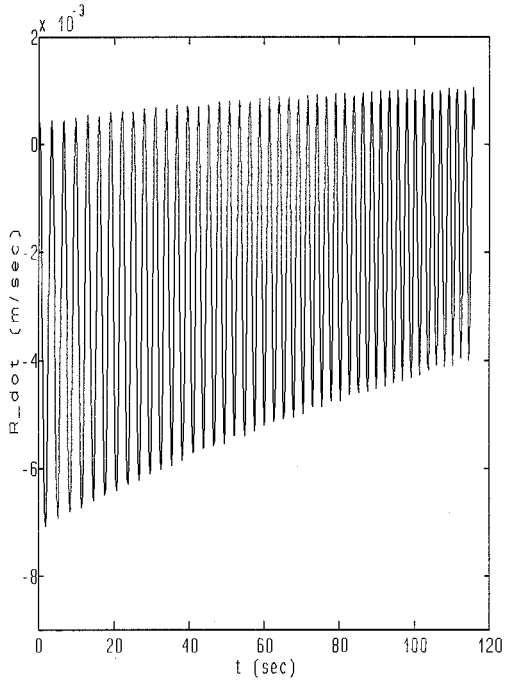

Figure 8. Radial velocity $\dot{R}$ (linear model).

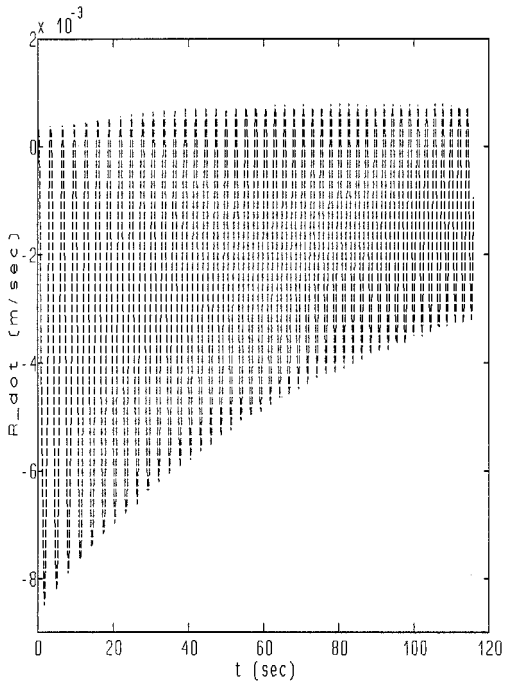

Figure 9. Radial velocity $\dot{R}$ (quadratic model).

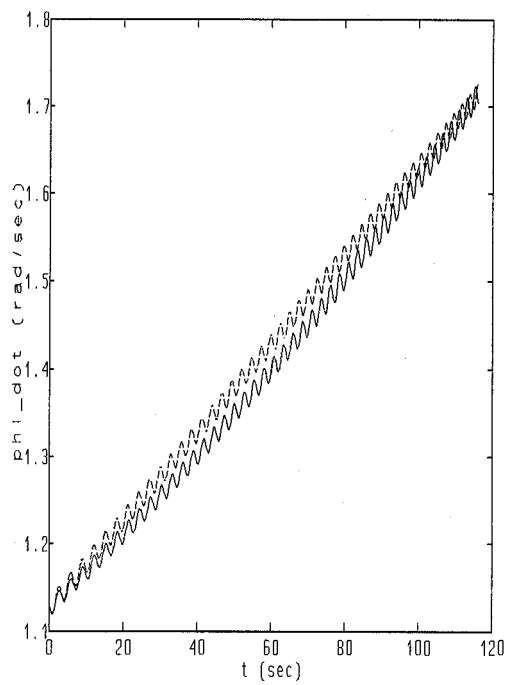

Figure 10. Angular velocity $\dot{\varphi}$.

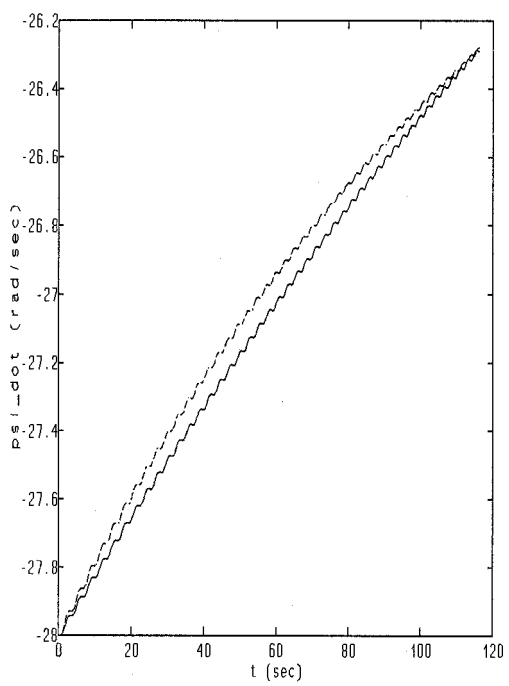

Figure 11. Spin $\dot{\psi}$.

With all of the above data we have run the Runge-Kutta routine ODE45.M, supplied by the mathematical software package 386-MATLAB, where we set the error tolerance to 10^{-6}. The results are reported in Figures 6–11, where the dashed graphs represent the output from the quadratic friction model. Figure 6 shows an almost linearly evolving total covered angle φ for both models. Therefore, and because the ball moves in orbit round the centre of the drum, we will often consider the solution as a function of φ, rather than of t. A more natural way to observe the motion of the ball – especially from a player's point of view – is thus depicted in Figure 7. It shows that the ball slowly spirals down the drum, with clearly perceptible elliptical revolutions. The distance to the centre of the drum decreases slightly faster in the quadratic case, as does the amplitude of the corresponding oscillations (see Figures 8 and 9). Finally, the angular velocity of the ball shows a gradual though oscillatory increase, whereas the spin gradually decreases (see Figures 10 and 11). Although the two friction models lead to different results, the overall characteristics appear to be very similar. We prefer to work with the linear model. Our reasons for this preference will be stated in the next section.

4. Analytical solutions

4.1. Rescaling the equations

In this section – as in the previous one – we neglect the spin resistance ($h = 0$), and assume that the drum is in a perfectly horizontal position ($\beta = 0$). Hence the motion of the ball depends on the gravitational force (magnitude: F_g) and the resistive force (F_a), the latter being much smaller than the former (see Section 2). This firstly gives us the opportunity to introduce a small parameter in terms of the ratio F_a/F_g. Secondly, this ratio makes it plausible to introduce two different time scales for the global motion of the ball:

(1) a typical time scale for one revolution, which is of the order $R/V_o \approx 1$ sec. This is in accordance with the fact, noted in Section 2, that the gravitational force F_g and the centrifugal force F_c are of the same order of magnitude;
(2) a time scale much larger than the first one, characteristic for the elapsed time after which the air drag becomes significant, of the order (see (28)[2,4]) of $7m/5\mathcal{F} = 7/5f \approx 100$ sec, due to the fact that the resistive force F_a is much smaller than both F_g and F_c.

On the basis of these two time scales we shall employ a two-variable expansion procedure as described in [6], Chapter 3.

To rescale the equations of motion (22), we introduce the dimensionless variables

$$\begin{aligned}
&\hat{R} = R/R_0, \qquad (R_0 = R(0)); \qquad \hat{\omega} = \dot{\varphi}/\omega_0, \qquad (\omega_0 = \dot{\varphi}(0));\\
&\hat{\Omega} = \dot{\psi}/\Omega_0, \quad \left(\Omega_0 = -\dot{\psi}(0) = \frac{1-\sin\alpha}{a\cos\alpha}R_0\omega_0\right); \qquad \hat{t} = \omega_0 t; \qquad (44)\\
&\hat{f} = \tfrac{5}{7}f_l/\omega_0; \qquad \hat{g} = \tfrac{5}{7}g\sin\alpha\cos\alpha/({\omega_0}^2R_0) = 1 - \tfrac{2}{7}\sin\alpha - \tfrac{5}{7}\sin^2\alpha,
\end{aligned}$$

where we again (see Sections 2 and 3) express our preference for a linear F_a-model, since it simplifies our analytic expressions. So from now on we assume $f(v_o)$ to equal a constant f_l. The new variables, with $h = \beta = 0$, change system (22) into

$$\frac{\mathrm{d}^2\hat{R}}{\mathrm{d}\hat{t}^2} = -\hat{f}\frac{\mathrm{d}\hat{R}}{\mathrm{d}\hat{t}} + \hat{R}\hat{\omega}^2\cos^2\alpha - \tfrac{2}{7}\hat{\omega}\hat{\Omega}(1-\sin\alpha)\sin\alpha - \hat{g},$$

$$\frac{\mathrm{d}\hat{\omega}}{\mathrm{d}\hat{t}} = -\hat{f}\hat{\omega} - 2\hat{R}^{-1}\hat{\omega}\frac{\mathrm{d}\hat{R}}{\mathrm{d}\hat{t}}, \qquad \frac{\mathrm{d}\hat{\Omega}}{\mathrm{d}\hat{t}} = \frac{\sin\alpha}{1-\sin\alpha}\hat{\omega}\frac{\mathrm{d}\hat{R}}{\mathrm{d}\hat{t}}, \tag{45}$$

with

$$\hat{R}(0) = \hat{\omega}(0) = \hat{\Omega}(0) = 1, \quad \text{and} \quad \frac{\mathrm{d}\hat{R}}{\mathrm{d}\hat{t}}(0) = 0. \tag{46}$$

When air resistance is completely neglected (*i.e.* $\mathcal{F}(v_o) = f(v_o) = f_l = 0$), the equations of motion admit three first integrals, representing conservation of angular momentum – about two distinct axes – and conservation of energy. With $\hat{f} = 0$, (45) reduces to (we omit the hats):

$$\ddot{R} = R\omega^2\cos^2\alpha - \tfrac{2}{7}\omega\Omega\sin\alpha(1-\sin\alpha) - g, \tag{47}$$

$$\dot{\omega} = -2R^{-1}\omega\dot{R}, \tag{48}$$

$$\dot{\Omega} = \sin\alpha(1-\sin\alpha)^{-1}\omega\dot{R}. \tag{49}$$

From (48) we find

$$\frac{\mathrm{d}}{\mathrm{d}t}\{R^2\omega\} = 0, \tag{50}$$

reflecting conservation of angular momentum about the central axis of the drum. Combination of (48) and (49) leads to conservation of angular momentum about the axis of spin, or

$$\frac{\mathrm{d}}{\mathrm{d}t}\{\Omega(1-\sin\alpha) + \omega R\sin\alpha\} = 0. \tag{51}$$

Another quantity that is preserved in the absence of air friction is the total mechanical energy, being the sum of kinetic and potential energies. We will, however, not use this quantity here, because it would – due to the essential nonlinear nature of the energy – needlessly complicate our calculations.

The two remaining conservation laws imply that the most direct way to study the dependency on $\hat{f}$ is by analyzing the momentary changes in the two physical quantities in (50) and (51). To this end, we introduce three new variables

$$y_1 = \hat{R}^2\hat{\omega}, \qquad y_2 = \hat{\Omega}(1-\sin\alpha) + \hat{\omega}\hat{R}\sin\alpha, \qquad y_3 = \hat{R}, \tag{52}$$

which results in the following form of the equations of motion:

$$\begin{aligned} \dot{y}_1 &= -\hat{f}y_1, \\ \dot{y}_2 &= \hat{f}y_1{y_3}^{-1}\sin\alpha, \\ \ddot{y}_3 &= -\hat{f}\dot{y}_3 + (1-\tfrac{5}{7}\sin^2\alpha){y_1}^2{y_3}^{-3} - \tfrac{2}{7}y_1y_2{y_3}^{-2}\sin\alpha - \hat{g}, \end{aligned} \tag{53}$$

and the initial conditions

$$y_1(0) = y_2(0) = y_3(0) = 1, \qquad \dot{y}_3(0) = 0. \tag{54}$$

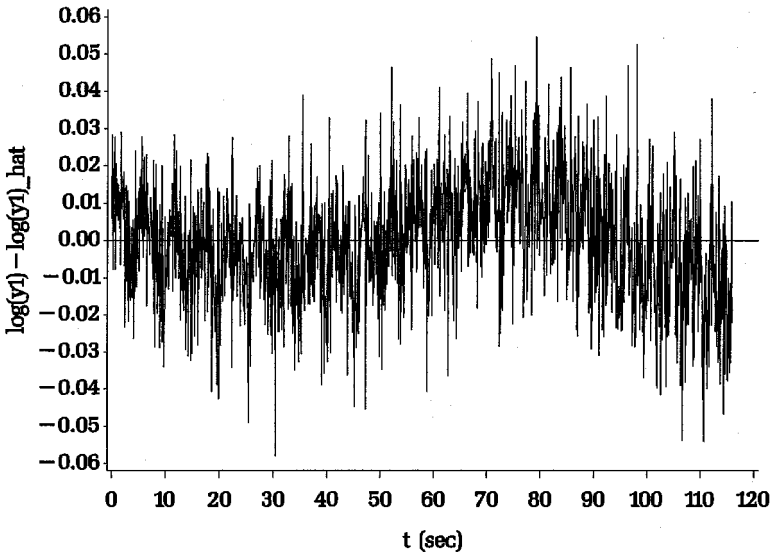

Figure 12. Residuals from the fitted regression equation $\log(y_1) = b_0 + b_1 t$, with $y_1 = R^2\dot{\varphi}$.

The first equation in (53) is uncoupled from the rest of the system, and leads – via the corresponding initial condition in (54) – to the solution

$$y_1 = \mathrm{e}^{-\hat{f}\hat{t}} = \mathrm{e}^{-5/7 f_l t}. \tag{55}$$

This formula expresses the explicit dependency of the total area covered per unit time $R^2\dot{\varphi}$ on the air friction coefficient f_l and time t. By fitting equation (55) to the experimental data provided by [1], we can expect to obtain an accurate estimate of coefficient f_l. A logarithmic transformation and a simple linear regression model, applied to orbit T11B21, yield the estimated value

$$\widehat{f_l} = 0{\cdot}014\,\mathrm{sec}^{-1}. \tag{56}$$

Note that this value does not differ much from the one in (42). The residuals from the regression model are plotted in Figure 12. The apparently small values indicate a close fit, but the rough sine shape does not indicate a truly linear friction model. But it also does not point to a truly quadratic model, as can be seen in Figure 13, where we used the earlier estimates of f_l and f_q to plot $\log(y_1)$ for both friction models (the dashed curve represents the quadratic model). We now definitely favour the linear model, because of its elegance and greater simplicity.

Substitution of the estimated f_l in (56) into the Runge-Kutta procedure does, however, not lead to an orbit that closely matches the example orbit T11B21. One of the obvious reasons is that the experimentally determined initial angular velocity appears to be lower than the theoretical value of 1·13 rad/sec in (36): [1] reports the value

$$\widehat{\omega_0} = 1{\cdot}09\,\mathrm{rad/sec}. \tag{57}$$

Figure 14 compares orbit T11B21 to the Runge-Kutta output based on the newly estimated values of f_l and ω_0 (the dashed graph represents the Runge-Kutta output). The overall shape of

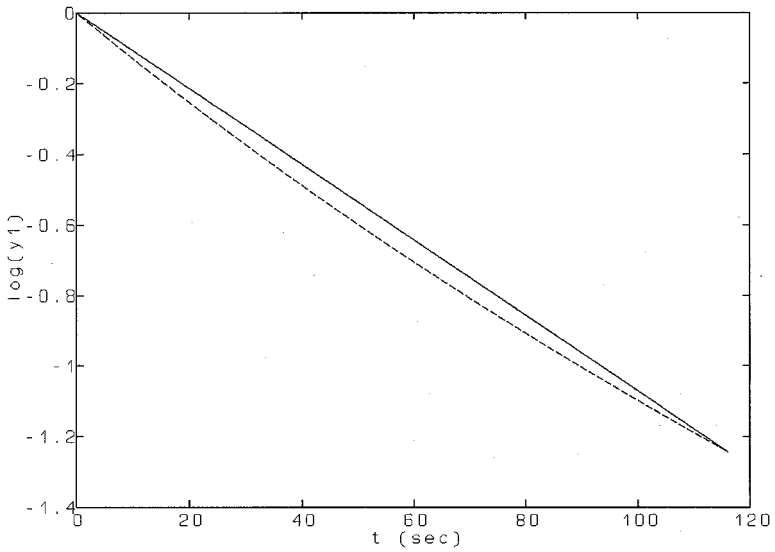

Figure 13. $\log(y_1)$ as function of t.

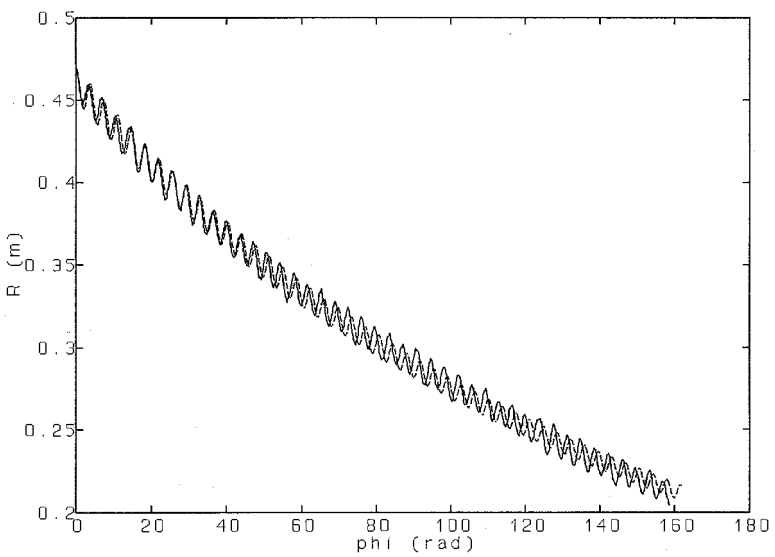

Figure 14. A comparison of numerical results and experimental data.

the graphs appears to be quite similar, especially during the first part of the experiment. However, the second part shows a slightly varying phase shift and a small variation in amplitude. We would be able to assess the influence of the system parameters and the initial conditions on the orbit of the ball better if we supplied system (45) with an analytical solution. But since such a solution is not available, we are forced to use an asymptotic approximation method. In the next subsection we will present such a method, where the asymptotics will be based on the small value of f_l, or (better) $\hat{f}$.

4.2. ASYMPTOTIC SOLUTIONS

Since the ball moves in an orbit around the centre of the drum, it is only natural to replace independent variable $\hat{t}$ in system (53) with the variable φ. This change of variables is common in the treatment of satellite equations (*cf.* [6], Section 3.4), which have a lot in common with our set of equations. The procedure we shall follow runs more or less along lines analogous to those presented in Sections 3.4.1 and 3.4.2 of [6].

With the transformations

$$u(\varphi) = {y_3}^{-1}, \qquad v(\varphi) = {y_1}^{-1}, \tag{58}$$

we find from (52)

$$\hat{\omega} = \frac{\mathrm{d}\varphi}{\mathrm{d}\hat{t}} = \frac{u^2}{v}. \tag{59}$$

Furthermore, to remove the factor $\sin\alpha$ in (53)[2], we rewrite y_2 as

$$y_2 = 1 - w(\varphi)\sin\alpha. \tag{60}$$

This change of variables transforms (53) into the new system

$$\begin{aligned} &\frac{\mathrm{d}v}{\mathrm{d}\varphi} = \hat{f}\frac{v^2}{u^2}, \qquad \frac{\mathrm{d}w}{\mathrm{d}\varphi} = \hat{f}\frac{1}{u}, \\ &\frac{\mathrm{d}^2u}{\mathrm{d}\varphi^2} = -u + \frac{v^2}{u^2} - \tfrac{2}{7}\sin\alpha\left(\frac{v^2}{u^2} - v\right) + \tfrac{5}{7}\sin^2\alpha\left(u - \frac{v^2}{u^2} - \tfrac{2}{5}vw\right), \end{aligned} \tag{61}$$

with corresponding initial conditions

$$u(0) = v(0) = 1, \qquad w(0) = 0, \qquad \frac{\mathrm{d}u}{\mathrm{d}\varphi}(0) = 0. \tag{62}$$

This new set of equations reveals an explicit dependence on just two dimensionless parameters, namely $\hat{f}$ and $\sin\alpha$, which both turn out to be small. The first one expresses, as we have seen before, the smallness of the resistive force as compared to the gravitational force (cf. [6], Sect. 3.4.2). We here replace $\hat{f}$ by ε and note that

$$\varepsilon = \hat{f} = \tfrac{5}{7}f_l/\omega_0 \approx 8{\cdot}8 \times 10^{-3} \tag{63}$$

in accordance with (36)[3] and the estimate for f_l in (56). The second small parameter is due to deviations in the gravitational force, related to the slope of the drum surface (comparable to [6], Sect. 3.4.1). Although the two small parameters have quite different physical origins, their influences on the equations of motion (61) are of the same order of magnitude. This is manifested as follows

$$\tfrac{2}{7}\sin\alpha = d_1\varepsilon, \qquad \tfrac{5}{7}\sin^2\alpha = d_2\varepsilon, \tag{64}$$

where d_1 and d_2 are coefficients of $O(1)$-magnitude, *i.e.* (from (34))

$$d_1 = 2{\cdot}69 \quad \text{and} \quad d_2 = 0{\cdot}559. \tag{65}$$

In this way we are able to combine the two small effects in one small parameter ε. With these substitutions, (61) can be rewritten as

$$\begin{aligned} &\frac{\mathrm{d}v}{\mathrm{d}\varphi} = \varepsilon\frac{v^2}{u^2}, \qquad \frac{\mathrm{d}w}{\mathrm{d}\varphi} = \varepsilon\frac{1}{u}, \\ &\frac{\mathrm{d}^2u}{\mathrm{d}\varphi^2} + u - \frac{v^2}{u^2} = \varepsilon\left[d_1\left(v - \frac{v^2}{u^2}\right) + d_2\left(u - \frac{v^2}{u^2} - \tfrac{2}{5}vw\right)\right]. \end{aligned} \tag{66}$$

Hence, u obeys the equation of a weakly nonlinear oscillator (*cf.* [6]), and this type of problem is well adapted to solution by the multiple-variable expansion method. As we already saw before, this problem involves two time scales, and therefore – following [6], Section 3.2 – we introduce the fast and slow φ-scale by

$$\varphi_1 = (1 + \varepsilon^2\omega_2 + \varepsilon^3\omega_3 + \cdots)\varphi \tag{67}$$

and

$$\varphi_2 = \varepsilon\varphi, \tag{68}$$

respectively, where $\omega_2, \omega_3, \ldots$, are unknown coefficients (not depending on ε). However, as we are not looking for a solution valid for all possible values of φ, but only for a range up to $\varphi = O(\varepsilon^{-1})$ (see Figure 6), these ω_i-coefficients are redundant here, and may be taken zero, i.e.

$$\omega_2 = \omega_3 = \cdots = 0 \Rightarrow \varphi_1 = \varphi. \tag{69}$$

Furthermore, we assume the variables $u,\ v$ and w to be functions of both φ_1 and φ_2, and write them as

$$u = u(\varphi_1, \varphi_2), \qquad v = v(\varphi_1, \varphi_2), \qquad w = w(\varphi_1, \varphi_2), \tag{70}$$

thus finally transforming (66) into

$$\begin{aligned} &\frac{\partial v}{\partial\varphi_1} + \varepsilon\frac{\partial v}{\partial\varphi_2} = \varepsilon\frac{v^2}{u^2}, \qquad \frac{\partial w}{\partial\varphi_1} + \varepsilon\frac{\partial w}{\partial\varphi_2} = \varepsilon\frac{1}{u}, \\ &\frac{\partial^2 u}{\partial{\varphi_1}^2} + 2\varepsilon\frac{\partial^2 u}{\partial\varphi_1\partial\varphi_2} + \varepsilon^2\frac{\partial^2 u}{\partial{\varphi_2}^2} = -u + \frac{v^2}{u^2} + \varepsilon\left[d_1 v + d_2 u - (d_1 + d_2)\frac{v^2}{u^2} - \tfrac{2}{5}d_2 vw\right]. \end{aligned} \tag{71}$$

Without loss of generality we may assume $\varphi_1(0) = \varphi_2(0) = 0$, yielding the initial conditions

$$\begin{aligned} &u(0,0) = v(0,0) = 1, \qquad w(0,0) = 0, \\ &\frac{\partial u}{\partial\varphi_1}(0,0) + \varepsilon\frac{\partial u}{\partial\varphi_2}(0,0) = 0. \end{aligned} \tag{72}$$

We now expand $u,\ v$, and w into the following asymptotic power series

$$u \sim \sum_{i=0}^{\infty} u_i(\varphi_1, \varphi_2)\varepsilon^i, \qquad v \sim \sum_{i=0}^{\infty} v_i(\varphi_1, \varphi_2)\varepsilon^i, \qquad w \sim \sum_{i=0}^{\infty} w_i(\varphi_1, \varphi_2)\varepsilon^i \tag{73}$$

and we shall try to find solutions for $u_i,\ v_i$, and w_i – on a limited φ-scale of $O(\varepsilon^{-1})$ – by substituting the series (73) in (71) and (72), and by matching the terms with equal powers in ε.

For the ε^0-terms we thus obtain

$$\frac{\partial v_0}{\partial \varphi_1} = 0, \qquad \frac{\partial w_0}{\partial \varphi_1} = 0, \qquad \frac{\partial^2 u_0}{\partial \varphi_1^2} = -u_0 + \frac{{v_0}^2}{{u_0}^2}, \tag{74}$$

with

$$\begin{aligned} &u_0(0,0) = v_0(0,0) = 1, \qquad w_0(0,0) = 0, \\ &\frac{\partial u_0}{\partial \varphi_1}(0,0) = 0, \end{aligned} \tag{75}$$

whereas the ε^1-terms yield

$$\begin{aligned} &\frac{\partial v_1}{\partial \varphi_1} = -\frac{\partial v_0}{\partial \varphi_2} + \frac{{v_0}^2}{{u_0}^2}, \\ &\frac{\partial w_1}{\partial \varphi_1} = -\frac{\partial w_0}{\partial \varphi_2} + \frac{1}{u_0}, \\ &\frac{\partial^2 u_1}{\partial {\varphi_1}^2} + 2\frac{\partial^2 u_0}{\partial \varphi_1 \partial \varphi_2} = -u_1 + 2\left(\frac{v_0 v_1}{{u_0}^2} - \frac{{v_0}^2 u_1}{{u_0}^3}\right) + d_1 v_0 + d_2 u_0 \\ &\qquad\qquad - (d_1 + d_2)\frac{{v_0}^2}{{u_0}^2} - \tfrac{2}{5} d_2 v_0 w_0, \end{aligned} \tag{76}$$

with

$$\begin{aligned} &u_1(0,0) = v_1(0,0) = w_1(0,0) = 0, \\ &\frac{\partial u_1}{\partial \varphi_1}(0,0) + \frac{\partial u_0}{\partial \varphi_2}(0,0) = 0. \end{aligned} \tag{77}$$

From (74)^3, with initial conditions (75), we find that both the first and the second derivative of u_0, with respect to φ_1, vanish in 0. From a quadrature of this equation it then follows that $\partial u_0/\partial \varphi_1 = 0$ for all $\varphi_1 > 0$, and hence we obtain from (74)

$$u_0 = U_0(\varphi_2), \qquad v_0 = V_0(\varphi_2), \qquad w_0 = W_0(\varphi_2), \tag{78}$$

such that

$${U_0}^3(\varphi_2) = {V_0}^2(\varphi_2) \tag{79}$$

and

$$U_0(0) = V_0(0) = 1, \qquad W_0(0) = 0. \tag{80}$$

Solutions for U_0, V_0 and W_0 follow from the ε^1-equations by requiring that the secular terms must equal zero (*cf.* [6]). So the first equation in (76) yields

$$\frac{\partial v_1}{\partial \varphi_1} = -\frac{\mathrm{d}V_0}{\mathrm{d}\varphi_2} + \frac{{V_0}^2}{{U_0}^2} = -{V_0}' + {V_0}^{2/3} \tag{81}$$

which would result in a linear, unbounded particular solution for v_1, unless

$$-{V_0}' + {V_0}^{2/3} = 0, \tag{82}$$

yielding, with $V_0(0) = 1$,

$$V_0 = (1 + \tfrac{1}{3}\varphi_2)^3 \tag{83}$$

and

$$U_0 = (1 + \tfrac{1}{3}\varphi_2)^2. \tag{84}$$

Analogously, the second equation in (74) leads us to

$$\frac{\partial w_1}{\partial \varphi_1} = -\frac{\mathrm{d}W_0}{\mathrm{d}\varphi_2} + \frac{1}{U_0} = -{W_0}' + (1 + \tfrac{1}{3}\varphi_2)^{-2}, \tag{85}$$

or, with $W_0(0) = 0$,

$$W_0 = \varphi_2(1 + \tfrac{1}{3}\varphi_2)^{-1}. \tag{86}$$

Hence we see that for a complete solution of the ε^0-terms, we need the equations of the ε^1-approximation (and so on for the higher-order terms). Substitution of (83), (84) and (86) in (76) results in

$$\begin{aligned} &\frac{\partial v_1}{\partial \varphi_1} = 0, \quad \text{or} \quad v_1 = V_1(\varphi_2), \\ &\frac{\partial w_1}{\partial \varphi_1} = 0, \quad \text{or} \quad w_1 = W_1(\varphi_2) \end{aligned} \tag{87}$$

and (where the last two results have already been substituted)

$$\frac{\partial^2 u_1}{\partial {\varphi_2}^2} + 3u_1 = \tfrac{1}{3}(d_1 - \tfrac{6}{5}d_2)\varphi_2(1 + \tfrac{1}{3}\varphi_2)^2 + 2(1 + \tfrac{1}{3}\varphi_2)^{-1}V_1 =: R_1(\varphi_2). \tag{88}$$

The solution of the latter equation reads

$$u_1(\varphi_1, \varphi_2) = U_1(\varphi_2) + A_1(\varphi_2)\sin\sqrt{3}\varphi_1 + B_1(\varphi_2)\cos\sqrt{3}\varphi_1, \tag{89}$$

with

$$U_1(\varphi_2) = \tfrac{1}{3}R_1(\varphi_2), \tag{90}$$

and, following from (77) and $R_1(0) = 0$,

$$A_1(0) = -\tfrac{2}{9}\sqrt{3}, \qquad B_1(0) = 0. \tag{91}$$

We can determine the functions A_1, B_1, V_1, and W_1 by matching the ε^2-terms, and equating the secular terms (which lead to unbounded solutions in φ_1) to zero. This eventually leads to an explicit expression for the apparently periodic function u_1.

The ε^2-versions of the first two equations in (71) lead to

$$\begin{aligned}
\frac{\partial v_2}{\partial \varphi_1} &= \left[-\frac{\mathrm{d}V_1}{\mathrm{d}\varphi_2} + 2(1+\tfrac{1}{3}\varphi_2)^{-1}V_1 - \tfrac{2}{3}R_1\right] \\
&\quad -2A_1 \sin\sqrt{3}\varphi_1 - 2B_1\cos\sqrt{3}\varphi_1, \quad (v_2(0,0) = 0), \\
\frac{\partial w_2}{\partial \varphi_1} &= \left[-\frac{\mathrm{d}W_1}{\mathrm{d}\varphi_2} - \tfrac{1}{3}(1+\tfrac{1}{3}\varphi_2)^{-4}R_1\right] \\
&\quad -(1+\tfrac{1}{3}\varphi_2)^{-4}(A_1\sin\sqrt{3}\varphi_1 + B_1\cos\sqrt{3}\varphi_1), \quad (w_2(0,0) = 0).
\end{aligned} \tag{92}$$

The solutions remain bounded only if the secular terms (between square brackets) are equal to zero, hence

$$V_1{}' - 2(1+\frac{1}{3}\varphi_2)^{-1}V_1 = -\frac{2}{3}R_1, \qquad W_1{}' = -\frac{1}{3}(1+\frac{1}{3}\varphi_2)^{-4}R_1, \tag{93}$$

which leads, via $V_1(0) = W_1(0) = 0$, and R_1 as in (88), to

$$V_1(\varphi_2) = -\tfrac{1}{9}(d_1 - \tfrac{6}{5}d_2){\varphi_2}^2(1+\tfrac{1}{3}\varphi_2)^2 \tag{94}$$

and

$$W_1(\varphi_2) = -\tfrac{1}{3}(d_1 - \tfrac{6}{5}d_2)\varphi_2(1+\tfrac{2}{3}\varphi_2)(1+\tfrac{1}{3}\varphi_2)^{-2} + (d_1 - \tfrac{6}{5}d_2)\log(1+\tfrac{1}{3}\varphi_2). \tag{95}$$

By substituting these results in (92) and solving the resulting differential equations, we obtain

$$v_2(\varphi_1,\varphi_2) = V_2(\varphi_2) + \frac{2\sqrt{3}}{3}A_1\cos\sqrt{3}\varphi_1 - \frac{2\sqrt{3}}{3}B_1\sin\sqrt{3}\varphi_1, \tag{96}$$

with

$$V_2(0) = -\frac{2\sqrt{3}}{3}A_1(0) = \tfrac{4}{9} \tag{97}$$

and

$$w_2(\varphi_1,\varphi_2) = W_2(\varphi_2) + \frac{\sqrt{3}}{3}(1+\tfrac{1}{3}\varphi_2)^{-4}\{A_1\cos\sqrt{3}\varphi_1 - B_1\sin\sqrt{3}\varphi_1\} \tag{98}$$

with

$$W_2(0) = -\frac{\sqrt{3}}{3}A_1(0) = \tfrac{2}{9}. \tag{99}$$

The above results allow us to write out the ε^2-terms in (71)[3] as

$$\begin{aligned}\frac{\partial^2 u_2}{\partial {\varphi_1}^2} + 3u_2 \;=\; & R_2(\varphi_2) + \tfrac{3}{2}(1+\tfrac{1}{3}\varphi_2)^{-2}\{2A_1B_1\sin 2\sqrt{3}\varphi_1 - (A_1^2 - B_1^2)\cos 2\sqrt{3}\varphi_1\} \\ & -2\sqrt{3}[A_1' - \tfrac{2}{3}(1+\tfrac{1}{3}\varphi_2)^{-1}A_1 - \omega_1 B_1]\cos\sqrt{3}\varphi_1 \\ & +2\sqrt{3}[B_1' - \tfrac{2}{3}(1+\tfrac{1}{3}\varphi_2)^{-1}B_1 + \omega_1 A_1]\sin\sqrt{3}\varphi_1,\end{aligned} \tag{100}$$

where

$$\begin{aligned}R_2 = {} & (\tfrac{4}{27} + \tfrac{2}{9}d_1^2 + \tfrac{1}{5}d_1d_2 - \tfrac{14}{25}d_2^2)\varphi_2 + (\tfrac{2}{81} + \tfrac{4}{27}d_1^2 + \tfrac{2}{15}d_1d_2 - \tfrac{28}{75}d_2^2)\varphi_2^2 \\ & + \tfrac{11}{135}d_2(d_1 - \tfrac{6}{5}d_2)\varphi_2^3 - \tfrac{1}{81}(d_1 - \tfrac{6}{5}d_2)^2\varphi_2^4 \\ & - \tfrac{2}{5}d_2(d_1 - \tfrac{6}{5}d_2)(1+\tfrac{1}{3}\varphi_2)^3\log(1+\tfrac{1}{3}\varphi_2) + 2(1+\tfrac{1}{3}\varphi_2)^{-1}V_2(\varphi_2)\end{aligned} \tag{101}$$

and

$$\omega_1 = \frac{\sqrt{3}}{3}(d_1 + \tfrac{3}{2}d_2) + \frac{\sqrt{3}}{9}(d_1 - \tfrac{6}{5}d_2)\varphi_2. \tag{102}$$

In this case, the secular terms are the ones with $\cos\sqrt{3}\varphi_1$ and $\sin\sqrt{3}\varphi_1$. Equating these terms to zero, we find

$$A_1' = \frac{2}{3}(1+\frac{1}{3}\varphi_2)^{-1}A_1 + \omega_1 B_1, \qquad B_1' = \frac{2}{3}(1+\frac{1}{3}\varphi_2)^{-1}B_1 - \omega_1 A_1. \tag{103}$$

A straightforward solution of (103) subject to the initial conditions (91) yields

$$A_1(\varphi_2) = -\tfrac{2}{9}(1+\tfrac{1}{3}\varphi_2)^2\cos\Omega_1, \tag{104}$$

$$B_1(\varphi_2) = \tfrac{2}{9}(1+\tfrac{1}{3}\varphi_2)^2\sin\Omega_1, \tag{105}$$

where

$$\Omega_1 = \Omega_1(\varphi_2) = \int_0^{\varphi_2}\omega_1(\phi)\,\mathrm{d}\phi = \frac{\sqrt{3}}{3}(d_1 + \tfrac{3}{2}d_2)\varphi_2 + \frac{\sqrt{3}}{18}(d_1 - \tfrac{6}{5}d_2)\varphi_2^2. \tag{106}$$

This ultimately results in the following explicit solution for u_1

$$u_1 = \tfrac{1}{9}(d_1 - \tfrac{6}{5}d_2)\varphi_2(1 - \tfrac{1}{3}\varphi_2)(1+\tfrac{1}{3}\varphi_2) - \tfrac{2}{9}\sqrt{3}(1+\tfrac{1}{3}\varphi_2)^2\sin(\sqrt{3}\varphi_1 - \Omega_1(\varphi_2)). \tag{107}$$

This completes the solution up to and including the $O(\varepsilon^1)$-terms. The ε^2- and higher-order terms can be found by substitution of results for A_1 and B_1 in the expressions for u_2, v_2 and w_2, from which we can derive the ε^3-versions of our equations. We may then determine

the still unknown functions, such as V_1, W_1 etc., by equating the secular terms to zero. This process involves the same techniques as have been applied to the calculation of lower-order terms; the results are reported in Appendix A. We have compared our asymptotic results with the numerically computed results in Section 3. This comparison shows that the differences are indeed of order $10^{-6} = O(\varepsilon^{-3})$ for all $\varphi \in [0, \varphi_f]$, with $\varphi_f \approx 160$ rad. This corroborates the correctness of our assumptions. We leave the conclusions to the final section.

5. Conclusions

In a deterministic model, the orbit of the ball in the drum is completely determined by the equations of motion, which are represented by a set of ordinary differential equations (22) and initial conditions (25). Since this system contains at least two coefficients of unknown magnitude, an exact solution will not become available until these coefficients will have been accurately determined by means of complementary experiments. Under the assumption of linear air friction, part of the system of differential equations can be solved exactly. The resulting solution (55) can be employed to estimate the unknown air-friction coefficient, viz. by fitting this solution to the experimental data provided by [1]. We may obtain a rough impression of the total solution by substituting some preliminary estimates in a Runge-Kutta routine: the results in Figure 7 show a slightly elliptical, downward spiraling orbit. The slope of the descent and the periodicity of the elliptical spiral appear to be strongly dependent on the air-friction force (this follows directly from the formulas in Section 4). A reliable prediction of the outcome hence requires a very accurate estimate; further research will hopefully provide this estimate.

Under the assumption of a zerospin friction coefficient, the differential equations of (22) can be expressed in terms of only two dimensionless parameters: α and ε, where α is the angle of inclination of the drum surface, and ε is a simple combination of the air friction coefficient and the ball's initial angular velocity (see (63)). As has been shown in (65), these two small effects can be combined into one small parameter, for which we have taken ε. The smallness of ε physically represents the fact that the resistive force F_a, due to air friction, is much larger than both the gravitational force F_g and the centrifugal force F_c. When a linear air friction model is applied, the system of equations can be solved analytically through expansion of the solution into an asymptotic power series in ε. The definitions (52) and (58), together with the formulas in Appendix A, yield

$$\begin{aligned} u = R_0/R &= (1 + \tfrac{1}{3}\varphi_2)^2 + O(\varepsilon) \\ &= (1 + \tfrac{1}{3}\varepsilon\varphi)^2 + O(\varepsilon), \end{aligned} \tag{108}$$

which reveals explicitly a slowly descending orbit, the slope of which is largely determined by the value of ε. Higher-order approximations reveal an elliptical spiral

$$\begin{aligned} u = R_0/R &= (1 + \tfrac{1}{3}\varphi_2)^2 + \tfrac{1}{9}\varepsilon(d_1 - \tfrac{6}{5}d_2)(1 - \tfrac{1}{9}{\varphi_2}^2)\varphi_2 \\ &\quad - \frac{2\sqrt{3}}{9}\varepsilon(1 + \tfrac{1}{3}\varphi_2)^2 \sin(\sqrt{3}\varphi_1 - \Omega_1) + O(\varepsilon^2) \end{aligned}$$

$$= (1+\tfrac{1}{3}\varphi_2)^2\{1+\tfrac{1}{9}\varepsilon(d_1-\tfrac{6}{5}d_2)(3-\varphi_2)(3+\varphi_2)^{-1}\varphi_2\}$$

$$\times\left\{1-\frac{2\sqrt{3}}{9}\varepsilon\sin(\sqrt{3}\varphi_1-\Omega_1)\right\}+O(\varepsilon^2). \tag{109}$$

During one revolution, and to within $O(\varepsilon)$-approximation, φ_2 is constant, hence (109) strongly resembles the phase-plane equation of an ordinary ellipse,

$$1/r = 1/c\{1-e\sin\theta\}, \tag{110}$$

with the origin situated at one of the foci, and the major axis corresponding to $\theta=\pi/2$. Apart from a scaling factor, expression (109) represents an elliptical curve with an eccentricity of $2\sqrt{3}/9\varepsilon+O(\varepsilon^2)$. This curve is periodic with frequency $\sqrt{3}$.

If Golden Ten could be considered to be a deterministic game, then the outcome of the game would depend directly on the point where the ball leaves the rim, and the players could then predict the final outcome by accurately observing just this one point. The exact location of this point can however be quite hard to determine, since this requires an extrapolation technique. A more manageable strategy is to observe one or more points somewhere in the middle of the orbit: the accuracy of these observations can be increased by interpolating the pattern of rotating ellipses. The effectiveness of the prediction can be improved by making allowance for very small disturbances, which will eventually lead to a shift of one or two compartment numbers. However, if further research points out that a deterministic model does not suffice – as can in fact already be suspected from Figure 14 – the success of this strategy will be very meagre. Future research will have to decide the validity of the assumptions that were made so far. Guided by the asymptotic results in Section 4, we hope to attain more insight in the nature of possible disturbances, and how to include these as random factors in an extended model for the motion of the ball in the drum.

Appendix

A. Asymptotic power series

This appendix contains the coefficient lists of the power series in (73). We derived the formulas by employing the techniques described in Section 4.3. Most of the calculations were done with the software package Mathematica-386/7.

$$u_0 = (1+\tfrac{1}{3}\varphi_2)^2, \tag{A.1}$$

$$v_0 = (1+\tfrac{1}{3}\varphi_2)^3, \tag{A.2}$$

$$w_0 = \varphi_2(1+\tfrac{1}{3}\varphi_2)^{-1}, \tag{A.3}$$

$$u_1 = \tfrac{1}{9}(d_1-\tfrac{6}{5}d_2)\varphi_2(1-\tfrac{1}{3}\varphi_2)(1+\tfrac{1}{3}\varphi_2)-\frac{2\sqrt{3}}{9}(1+\tfrac{1}{3}\varphi_2)^2\sin(\sqrt{3}\varphi_1-\Omega_1), \tag{A.4}$$

$$v_1 = -\tfrac{1}{9}(d_1-\tfrac{6}{5}d_2){\varphi_2}^2(1+\tfrac{1}{3}\varphi_2)^2, \tag{A.5}$$

$$w_1 = -\tfrac{1}{3}(d_1-\tfrac{6}{5}d_2)\varphi_2(1+\tfrac{2}{3}\varphi_2)(1+\tfrac{1}{3}\varphi_2)^{-2}+(d_1-\tfrac{6}{5}d_2)\log(1+\tfrac{1}{3}\varphi_2), \tag{A.6}$$

$$u_2 = \tfrac{8}{27} + (\tfrac{8}{27} + \tfrac{2}{27}d_1^2 - \tfrac{1}{45}d_1d_2 - \tfrac{2}{25}d_2^2)\varphi_2 + (\tfrac{2}{81} - \tfrac{2}{45}d_1d_2 + \tfrac{4}{75}d_2^2)\varphi_2^2$$
$$-\tfrac{2}{243}(d_1 + \tfrac{27}{10}d_2)(d_1 - \tfrac{6}{5}d_2)\varphi_2^3\tfrac{1}{729}(d_1 - \tfrac{6}{5}d_2)^2\varphi_2^4$$
$$+\tfrac{2}{15}d_2(d_1 - \tfrac{6}{5}d_2)(1 + \tfrac{1}{3}\varphi_2)^3\log(1 + \tfrac{1}{3}\varphi_2)$$
$$-(1 + \tfrac{1}{3}\varphi_2)\{\lambda_1\sin(\sqrt{3}\varphi_1 - \Omega_1) + \lambda_2\cos(\sqrt{3}\varphi_1 - \Omega_1)\}$$
$$+\tfrac{2}{81}(1 + \tfrac{1}{3}\varphi_2)^2\cos(2\sqrt{3}\varphi_1 - 2\Omega_1), \tag{A.7}$$

$$v_2 = \{\tfrac{4}{9} + (\tfrac{10}{27} - \tfrac{2}{15}d_1d_2 + \tfrac{4}{25}d_2^2)\varphi_2 + (\tfrac{2}{81} - \tfrac{2}{27}d_1^2 - \tfrac{2}{15}d_1d_2 + \tfrac{4}{15}d_2^2)\varphi_2^2$$
$$-\tfrac{1}{81}(d_1 + 6d_2)(d_1 - \tfrac{6}{5}d_2)\varphi_2^3 + \tfrac{2}{243}(d_1 - \tfrac{6}{5}d_2)^2\varphi_2^4\}(1 + \tfrac{1}{3}\varphi_2)$$
$$+\tfrac{2}{5}(d_1 - \tfrac{6}{5}d_2)(1 + \tfrac{1}{3}\varphi_2)^4\log(1 + \tfrac{1}{3}\varphi_2)$$
$$-\tfrac{4}{9}(1 + \tfrac{1}{3}\varphi_2)^2\cos(\sqrt{3}\varphi_1 - \Omega_1), \tag{A.8}$$

$$w_2 = \{\tfrac{2}{9} - \tfrac{13}{15}d_2(d_1 - \tfrac{6}{5}d_2)\varphi_2 - (\tfrac{10}{81} + \tfrac{1}{27}d_1^2 + \tfrac{32}{45}d_1d_2 - \tfrac{68}{75}d_2^2)\varphi_2^2$$
$$-(\tfrac{14}{729} + \tfrac{23}{135}d_1d_2 - \tfrac{46}{225}d_2^2)\varphi_2^3\}(1 + \tfrac{1}{3}\varphi_2)^{-3}$$
$$+d_2(d_1 - \tfrac{6}{5}d_2)\{\tfrac{13}{5} - \tfrac{1}{5}\log(1 + \tfrac{1}{3}\varphi_2)\}\log(1 + \tfrac{1}{3}\varphi_2)$$
$$-\tfrac{2}{9}(1 + \tfrac{1}{3}\varphi_2)^{-2}\cos(\sqrt{3}\varphi_1 - \Omega_1), \tag{A.9}$$

$$\Omega_1 = \frac{\sqrt{3}}{3}(d_1 + \tfrac{3}{2}d_2)\varphi_2 + \frac{\sqrt{3}}{18}(d_1 - \tfrac{6}{5}d_2)\varphi_2^2, \tag{A.10}$$

$$\lambda_1 = \frac{\sqrt{3}}{9}(d_1 + \tfrac{3}{5}d_2) + \frac{2\sqrt{3}}{27}(d_1 - \tfrac{3}{10}d_2)\varphi_2 - \frac{\sqrt{3}}{243}(d_1 - \tfrac{6}{5}d_2)\varphi_2^2$$
$$+\frac{2\sqrt{3}}{45}d_2(1 + \tfrac{1}{3}\varphi_2)\log(1 + \tfrac{1}{3}\varphi_2), \tag{A.11}$$

$$\lambda_2 = \tfrac{26}{81} - (\tfrac{2}{243} + \tfrac{1}{27}d_1^2 + \tfrac{7}{45}d_1d_2 + \tfrac{3}{100}d_2^2)\varphi_2$$
$$+(\tfrac{2}{729} - \tfrac{1}{81}d_1^2 - \tfrac{5}{54}d_1d_2 + \tfrac{7}{180}d_2^2)\varphi_2^2$$
$$+\tfrac{1}{243}(d_1 - \tfrac{9}{2}d_2)(d_1 - \tfrac{5}{6}d_2)\varphi_2^3 + \tfrac{1}{729}(d_1 - \tfrac{6}{5}d_2)^2\varphi_2^4$$
$$+\tfrac{2}{15}d_2(d_1 - \tfrac{6}{5}d_2)(1 + \tfrac{1}{3}\varphi_2)^3\log(1 + \tfrac{1}{3}\varphi_2). \tag{A.12}$$

References

1. J.C. De Vos, *A thousand Golden Ten orbits.* Tilburg University (1994) 80 pp.
2. B.B. Van der Genugten and P.E.M. Borm, Golden-Ten: een kans- of behendigheidsspel. *Kwantitatieve Methoden* 38 (1991) 61–80.
3. P.W. Likins, *Elements of Engineering Mathematics.* New York: McGraw-Hill (1973) 538 pp.
4. H.L. Dryden, F.P. Murnaghan, and H. Bateman, *Hydrodynamics.* New York: Dover Publications (1956) 634 pp.
5. H. Rouse, *Elementary Mechanics of Fluids.* New York: John Wiley and Sons (1959) 376 pp.
6. J. Kevorkian and J.D. Cole, *Perturbation Methods in Applied Mathematics.* New York: Springer (1981) 558 pp.